

Quantum Zeno manipulation of quantum dots

N. Ahmadiiaz¹, M. Geller², J. König², P. Kratzer², A. Lorke², G. Schaller¹, and R. Schützhold^{1,3}¹Helmholtz-Zentrum Dresden-Rossendorf, Bautzner Landstraße 400, 01328 Dresden, Germany²Fakultät für Physik and CENIDE, Universität Duisburg-Essen, Lotharstraße 1, 47057 Duisburg, Germany³Institut für Theoretische Physik, Technische Universität Dresden, 01062 Dresden, Germany

(Received 19 April 2022; accepted 26 August 2022; published 26 September 2022)

We investigate whether and how the quantum Zeno effect, i.e., the inhibition of quantum evolution by frequent measurements, can be employed to isolate a quantum dot from its surrounding electron reservoir. In contrast to the often studied case of tunneling between discrete levels, we consider the tunneling of an electron from a continuum reservoir to a discrete level in the dot. Realizing the quantum Zeno effect in this scenario can be much harder because the measurements should be repeated before the wave packet of the hole left behind in the reservoir moves away from the vicinity of the dot. Thus the required repetition rate could be lowered by having a flat band (with a slow group velocity) in resonance with the dot or a sufficiently small Fermi velocity or a strong external magnetic field. We also consider the anti-Zeno effect, i.e., how measurements can accelerate or enable quantum evolution.

DOI: [10.1103/PhysRevResearch.4.L032045](https://doi.org/10.1103/PhysRevResearch.4.L032045)

Introduction. One of the major distinctions between classical and quantum physics is the role of measurements. As a consequence, it is impossible to directly observe quantum evolution taking place without actually affecting it. A striking example is the quantum Zeno effect which describes slowing down or even stopping quantum evolution by frequent measurements, see, e.g., [1–7].

Let us discuss the basic picture by means of a simple example, two discrete states or levels $|1\rangle$ and $|2\rangle$ of equal energy which are tunnel coupled. Preparing the initial state in one level $|\Psi(t=0)\rangle = |1\rangle$, the time-dependent probability $P_2(t) = |\langle 2|\Psi(t)\rangle|^2$ for the other level reads $P_2(t) = \sin^2(\gamma t)$, where the frequency $\gamma > 0$ is given by the tunneling strength. For short times $t \ll 1/\gamma$, we obtain a quadratic growth $P_2(t) \approx \gamma^2 t^2$, because in quantum physics amplitudes instead of probabilities are added. However, if we measure the level occupation after such a short time, i.e., within the quadratic-growth regime, we project the state $|\Psi(t)\rangle$ back to the initial state $|1\rangle$ (assuming a strong, i.e., projective measurement) with high probability $P_1(t) \approx 1 - \gamma^2 t^2$, and thus the quantum evolution has to start again afterwards. In other words, the amplitudes before and after the measurement no longer interfere constructively, because we have obtained which-way information via the measurement. Now, repeating this measurement with a fast rate (much larger than γ) would effectively keep setting back the quantum evolution such that the quantum state stays in the initial level $|1\rangle$. This inhibition (or slowing down) of quantum evolution is usually referred

to as the quantum Zeno effect [1]. Note that this line of argument crucially relies on the quadratic growth $P_2(t) \approx \gamma^2 t^2$ discussed above. In case of a linear behavior $P_2(t) \sim t$, for example, setting back the evolution by measurements would not have this retarding effect.

The quantum Zeno effect is a striking example for quantum control [8–15] and closely related to passive quantum error correction schemes (similar to the spin-echo method). Thus this fascinating phenomenon is of fundamental interest and has already been observed experimentally in different systems, e.g., for ions in Penning traps [2], ultracold atoms in optical lattices [4,16], Bose-Einstein condensates in magnetic traps [5,14], Rydberg atoms in cavities [6], or superconducting qubits [7].

On much shorter timescales, electrons in quantum dots are also very suitable systems for studying the quantum Zeno effect. Their energy levels and tunneling rates can be manipulated (e.g., by the variation of voltages that are applied to suitably placed gate electrodes) or the size of the dot, and they have quite long coherence times, while their states can be read out, i.e., measured, quite quickly by capacitive charge detectors [17,18] or optical transitions [19,20], for example.

In most previous works, the quantum Zeno effect has been studied in a regime where the aforementioned picture based on transitions between discrete levels can be applied [2,3,21–25]. In the following we shall study the more involved case of transitions between a discrete level and a continuum (a Fermi gas or liquid), see also, e.g., Refs. [26,27]. As a concrete experimental realization, we consider a quantum dot coupled to a reservoir in the form of an effectively two-dimensional electron gas (2DEG) [28–32].

The model. We consider the quantum-dot-reservoir system in good approximation [33], being described by the following

Published by the American Physical Society under the terms of the Creative Commons Attribution 4.0 International license. Further distribution of this work must maintain attribution to the author(s) and the published article's title, journal citation, and DOI.

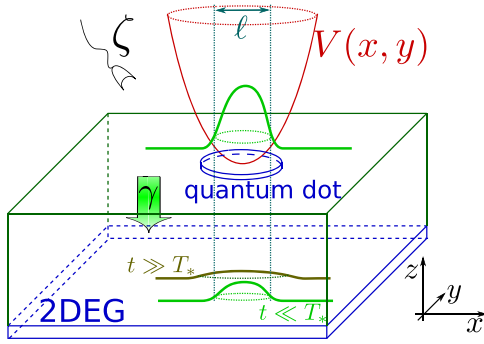


FIG. 1. Sketch of the quantum dot with confinement potential $V(x, y)$ coupled to the effectively two-dimensional electron gas (2DEG), both realized as lowest-quantum-well states. Tunneling with strength γ of an electron or hole wave packet with characteristic size ℓ from the dot to the 2DEG reservoir corresponds to discharging or charging. In the reservoir, the wave packets then spread or move away on a typical timescale T_* , which limits the repetition rate of the measurement (indicated by ζ) required for observing the quantum Zeno effect.

many-body Hamiltonian ($\hbar = 1$), cf. Fig. 1:

$$\hat{H} = \int d^2r \left(\frac{(\nabla \hat{\psi}_1^\dagger) \cdot (\nabla \hat{\psi}_1)}{2m} + V_1(x, y) \hat{\psi}_1^\dagger \hat{\psi}_1 + \frac{(\nabla \hat{\psi}_2^\dagger) \cdot (\nabla \hat{\psi}_2)}{2m} + (\gamma \hat{\psi}_1^\dagger \hat{\psi}_2 + \text{H.c.}) \right). \quad (1)$$

The first line represents the quantum dot for which we employ the standard [34] harmonic potential approximation $V_1(x, y) = V_0 + m\omega^2(x^2 + y^2)/2$, where the offset V_0 can be tuned by a gate voltage. The second line describes the reservoir and its tunnel coupling to the dot with the coupling strength γ . The field operators $\hat{\psi}_1(x, y)$ and $\hat{\psi}_2(x, y)$ could be envisaged as lowest-quantum-well states in z direction, for example, where we assume that the energies of the higher-quantum-well states are so large (tight confinement limit) that we can neglect them.

If we focus on the ground state of the quantum dot $\hat{\psi}_1(x, y) \rightarrow \Phi_0(x, y)\hat{a}_d$ and Fourier transform the reservoir modes $\hat{\psi}_2(x, y) \rightarrow \hat{\psi}_k$, the Hamiltonian (1) becomes

$$\hat{H} = \epsilon_d \hat{n}_d + \int d^2k [\epsilon_k \hat{\psi}_k^\dagger \hat{\psi}_k + (\gamma_k \hat{a}_d^\dagger \hat{\psi}_k + \text{H.c.})], \quad (2)$$

where ϵ_d denotes the energy of the quantum dot level and $\hat{n}_d = \hat{a}_d^\dagger \hat{a}_d$ the corresponding number operator, while $\epsilon_k = \mathbf{k}^2/(2m)$ are the single-particle energies of the reservoir modes $\mathbf{k} = (k_x, k_y)$. Finally, γ_k is determined by the Fourier transform of the ground-state wave function inside the quantum dot (see, e.g., [35]), i.e., Gaussian,

$$\gamma_k = \gamma \int \frac{d^2r}{2\pi} \Phi_0^*(x, y) e^{+i\mathbf{k}\cdot\mathbf{r}} = \gamma_0 \exp \left\{ -\frac{1}{2} \mathbf{k}^2 \ell^2 \right\}, \quad (3)$$

where $\ell = \sqrt{\hbar/(m\omega)}$ is the characteristic dot length scale. Note that the bilinear Hamiltonian (1) does not explicitly include nonlinear (e.g., Coulomb) interactions between the electrons nor their coupling to other degrees of freedom (e.g., phonons), whose potential impact will be discussed below.

Therefore we restrict ourselves to studying the transition between an empty and a singly occupied dot, for which a charging energy of the quantum dot is irrelevant.

Quantum-Zeno dynamics. Now we are in the position to study the tunneling process of an electron from the reservoir into the quantum dot. We start with the initial state $|\text{in}\rangle$ where the dot is empty $\hat{a}_d|\text{in}\rangle = 0$ while the reservoir is filled up to the Fermi energy.

Although the above model can be solved exactly using, e.g., Greens function techniques [36], we may already calculate the time-dependent probability $P(t)$ for the occupation of the quantum dot using standard time-dependent perturbation theory with respect to γ ,

$$P(t) = \langle \hat{n}_d(t) \rangle = 4 \int_F d^2k |\gamma_k|^2 \frac{\sin^2[(\epsilon_d - \epsilon_k)t/2]}{(\epsilon_d - \epsilon_k)^2}, \quad (4)$$

where the subscript F on the integral indicates that the integration runs up to Fermi energy ϵ_F .

Quantum-Zeno regime. Even within the region of applicability of perturbation theory (i.e., for small probabilities $P(t) \ll 1$), we obtain two temporal regimes. For small times t , the probability $P(t)$ grows quadratically:

$$P(t) = t^2 \int_F d^2k |\gamma_k|^2 + \mathcal{O}(t^3). \quad (5)$$

For the Gaussian case (3), this simplifies to

$$P(t) = \pi \frac{\gamma_0^2 t^2}{\ell^2} (1 - \exp\{-k_F^2 \ell^2\}) + \mathcal{O}(t^3), \quad (6)$$

where $k_F = \sqrt{2m\epsilon_F}$ denotes the Fermi momentum. If the Fermi energy ϵ_F is large enough, $2m\epsilon_F \ell^2 \gg 1$, i.e., $k_F^2 \ell^2 \gg 1$, we obtain $P(t) = \pi \gamma_0^2 t^2 / \ell^2$. In the opposite limit $k_F^2 \ell^2 \ll 1$, the integration is cut off by k_F^2 and we find $P(t) = \pi \gamma_0^2 t^2 k_F^2$.

Regime of Fermi's golden rule. For later times (but still in the perturbative regime $P(t) \ll 1$), we can use the standard approximation of the sinc function in Eq. (4) by a Dirac δ function and obtain a linear growth in time, consistent with Fermi's golden rule:

$$P(t) \approx 2\pi t \int_F d^2k |\gamma_k|^2 \delta(\epsilon_d - \epsilon_k). \quad (7)$$

Obviously, the above integral vanishes for $\epsilon_d > \epsilon_F$ and for $\epsilon_d < 0$, i.e., if there are no filled reservoir modes in resonance with the dot. (These cases are discussed in the Supplemental Material [37].) Assuming $\epsilon_F > \epsilon_d > 0$, we find for the Gaussian case (3) with $\epsilon_k = \mathbf{k}^2/(2m)$,

$$P(t) \approx (2\pi)^2 t m \gamma_0^2 \exp\{-2m\epsilon_d \ell^2\}. \quad (8)$$

The exponential suppression $\exp\{-2m\epsilon_d \ell^2\}$ for large dot energies $2m\epsilon_d \ell^2 \gg 1$ stems from the wave-function mismatch between the Gaussian ground-state wave function of the dot and the reservoir wave functions of the corresponding energy ϵ_d , which are rapidly oscillating for large ϵ_d . In order to avoid this suppression, we assume small dot energies $2m\epsilon_d \ell^2 \ll 1$ in the following.

As a peculiarity of the case of two spatial dimensions, the remaining prefactor $P(t) \approx (2\pi)^2 t m \gamma_0^2$ is actually independent of ϵ_d because the energy $\epsilon_k = \mathbf{k}^2/(2m)$ and the volume factor d^2k both display the same quadratic scaling in k , such that the density of states per energy is constant.

Crossover time. Having found an initial period of quadratic growth (5) for early times (quantum Zeno regime) followed by a period of linear growth (7) for later times (regime of Fermi's golden rule), we may estimate the crossover time T_* marking the transition between the two regimes [38] by comparing Eqs. (5) and (7). For the Gaussian limit we obtain with (6) and (8),

$$T_* \approx 4\pi m \ell^2 \frac{\exp\{-2m\epsilon_d \ell^2\}}{1 - \exp\{-\ell^2 k_F^2\}}. \quad (9)$$

Assuming small dot excitation energies $2m\epsilon_d \ell^2 \ll 1$ and considering the limiting cases as discussed after Eq. (6), this simplifies to $T_* \approx 4\pi m \ell^2$ for $\ell^2 k_F^2 \gg 1$ and to $T_* \approx 4\pi m/k_F^2$ for $\ell^2 k_F^2 \ll 1$, respectively.

As explained in the Introduction, only measurements with a repetition time faster than T_* can induce the quantum Zeno effect. This timescale is typically quite short and can be visualized by the following intuitive picture.

Let us first consider the case $\ell^2 k_F^2 \gg 1$. If an electron tunnels with a small amplitude from the reservoir to the quantum dot, it leaves behind a hole in the reservoir. The typical size of the initial wave packet of this hole is determined by the characteristic length ℓ of the ground-state wave function of the dot. Afterwards, this wave packet is spreading out or moving away with the typical group velocity at that length scale $v_{\text{group}} \propto 1/(\ell m)$. Once the wave packet has spread out too much or moved away too far, further tunneling amplitudes would not be added coherently and probabilities would add up instead. This is precisely the transition from the quantum Zeno regime to the regime of Fermi's golden rule occurring at the crossover time $T_* \sim \ell/v_{\text{group}}$.

In the opposite limit ($\ell^2 k_F^2 \ll 1$), one should just replace the length scale ℓ of the dot by the Fermi length $\ell_F \propto 1/k_F$ and the associated group velocity by the Fermi velocity $v_F = k_F/m$. Then, the crossover time T_* is basically the Fermi time T_F , which is related to the Fermi energy ϵ_F by Heisenberg's uncertainty relation [$T_* = \mathcal{O}(\epsilon_F^{-1})$] and determines the minimum response time of hole states in the reservoir.

Consistent with the results of [39], an effectively Markovian reservoir is obtained in the combined limit of $\ell \rightarrow 0$ and $k_F \rightarrow \infty$, where the available density of states in the reservoir becomes constant and the quantum Zeno regime or effect disappears $T_* = 0$.

General band structure. Let us now discuss possible generalizations of the above results (see also the Supplemental Material [37]). For reservoir electrons propagating in a lattice, the single-particle energies $\epsilon_{\mathbf{k}}$ of the reservoir modes \mathbf{k} should be replaced by the lattice band structure, which might also modify the (experimentally accessible [40]) couplings $\gamma_{\mathbf{k}}$ accordingly. Of course, the same would happen for non-harmonic quantum dot potentials $V_1(x, y) \neq V_0 + m\omega^2(x^2 + y^2)/2$. Nevertheless, one would still expect the effective Hamiltonian (2) to provide a good approximation. Thus the results (4) and thus (5) and (7) remain valid, but with modified $\epsilon_{\mathbf{k}}$ and $\gamma_{\mathbf{k}}$. This may entail interesting consequences. For example, if we have a flat band (with $\epsilon_{\mathbf{k}} = \text{const}$) below the Fermi energy in resonance with the quantum dot (i.e., $\epsilon_{\mathbf{k}} = \text{const} = \epsilon_d$), the probability (7) per time would become very large while the initial growth (5) would remain almost

unaffected since it is independent of $\epsilon_{\mathbf{k}}$. This means that the crossover time T_* would also become very large, which might help observing the quantum Zeno effect in this scenario. In terms of the intuitive picture sketched above, the group velocity becomes very small for such a flat band such that the wave packet stays quite long in the vicinity of the dot.

Magnetic field. The above finding regarding flat or nearly flat bands motivates the study of a strong external magnetic field perpendicular to the reservoir, because this also turns the reservoir modes into flat bands in the form of the well-known Landau levels.

As usual, we represent the constant perpendicular magnetic field $\mathbf{B} = B\mathbf{e}_z$ in the symmetric gauge by the vector potential $\mathbf{A} = \mathbf{B} \times \mathbf{r}/2$. Then, after minimal coupling $\nabla \rightarrow \nabla - q\mathbf{A}$ to the electron charge q , the Hamiltonian (1) acquires an additional angular-momentum contribution $-2\mathbf{A} \cdot \nabla = \mathbf{B} \cdot \hat{\mathbf{L}} = B\hat{L}_z$ as well as a harmonic confinement potential $V_B = \Omega_B^2(x^2 + y^2)/8$ from the quadratic term $\mathbf{A}^2 = B^2(x^2 + y^2)/4$, where Ω_B is the cyclotron frequency $\Omega_B = qB/m$.

Thus the reservoir eigenfunctions are no longer plane waves as in Eq. (2) but discrete Landau levels, which can be represented by the modes of a two-dimensional harmonic oscillator in polar coordinates r and φ [41]:

$$\psi_{n,l}(r, \varphi) = f_{n,l}(r)e^{il\varphi}. \quad (10)$$

Here $n \in \mathbb{N}$ and $l \in \mathbb{Z}$ are the quantum numbers corresponding to energy $\epsilon_n = \Omega_B(n + 1/2)$ and angular momentum \hat{L}_z , respectively. The radial mode functions $f_{n,l}(r)$ are given by polynomials multiplied by a Gaussian $\exp\{-r^2/(2\ell_B)^2\}$ with the magnetic length $\ell_B = 1/\sqrt{qB}$. For example, the lowest Landau levels with $n = 0$ have $f_{n=0,l}(r) \propto r^l \exp\{-r^2/(2\ell_B)^2\}$ with $l \geq 0$, which can be experimentally mapped [30,42].

The ground-state wave function of the quantum dot will also be modified, but merely by the additional harmonic confinement potential $V_B = \Omega_B^2(x^2 + y^2)/8$, which narrows the Gaussian wave function (i.e., decreases ℓ) and increases the energy ϵ_d . Since this wave function is rotationally symmetric (i.e., has zero angular momentum), it only tunnel couples to reservoir modes with $l = 0$.

If we now assume a strong magnetic field B and/or a small Fermi energy $\epsilon_F < 3\Omega_B/2$ such that only the lowest Landau levels are occupied, the effective Hamiltonian (2) can be restricted to the mode $n = l = 0$ and reads

$$\hat{H} = \epsilon_d \hat{n}_d + \frac{\Omega_B}{2} \hat{n}_{0,0} + (\gamma_{0,0} \hat{a}_d^\dagger \hat{a}_{0,0} + \text{H.c.}), \quad (11)$$

where the effective tunnel coupling $\gamma_{0,0}$ is determined by the overlap of the two Gaussian wave functions of the dot and $\psi_{0,0} \propto \exp\{-r^2/(2\ell_B)^2\}$.

Assuming resonance $\epsilon_d = \Omega_B/2$, this Hamiltonian (11) is then formally equivalent to tunneling between two discrete modes (described by \hat{a}_d and $\hat{a}_{0,0}$) such that we are back to the original picture of the quantum Zeno effect as described in the Introduction. Off-resonant scenarios $\epsilon_d \neq \Omega_B/2$ may give rise to the anti-Zeno effect [4,8,23,43], as discussed in the Supplemental Material [37].

Measurement model. So far, the Hamiltonian (1) only describes the internal dynamics of the electrons but not the actual

measurement process—which is causing the quantum Zeno effect. To incorporate this, let us construct a simple toy model for the readout. We assume that the dot is strongly illuminated by laser light (saturation regime), which quickly transfers the electron in the quantum dot from the ground-state level to an excited level $\hat{a}_e^\dagger \hat{a}_d$ as soon as the dot is occupied. This excited level then rapidly decays by emitting a photon as described by the bosonic creation and annihilation operators \hat{b}^\dagger and \hat{b} , where we focus on one mode for simplicity. Assuming that these excitation–deexcitation cycles occur much faster than all the other timescales considered above (e.g., T_*), we may use an effective description where the dot emits photons as soon as it is occupied. Thus we model the measurement by the additional Hamiltonian,

$$\hat{H}_{\text{measure}} = \hat{n}_d(i\zeta \hat{b}^\dagger + \text{H.c.}), \quad (12)$$

with the detector coupling strength $\zeta > 0$, which is basically a pointer Hamiltonian for measuring the observable \hat{n}_d .

Since \hat{H}_{measure} commutes with the undisturbed Hamiltonian $\hat{H}_0 = \epsilon_d \hat{n}_d + \int d^2k \epsilon_{\mathbf{k}} \hat{\psi}_{\mathbf{k}}^\dagger \hat{\psi}_{\mathbf{k}}$, we may incorporate it easily into the time-dependent perturbation theory used above for calculating $P(t)$. In the interaction picture, the dot annihilation operator \hat{a}_d just acquires an additional operator-valued factor,

$$\hat{a}_d(t) = e^{-i\epsilon_d t} \exp\{(\zeta \hat{b}^\dagger - \text{H.c.})t\} \hat{a}_d(0), \quad (13)$$

which represents the dynamics induced by $\hat{H}_0 + \hat{H}_{\text{measure}}$. When acting on the initial photonic vacuum state $|0\rangle$ with $\hat{b}|0\rangle = 0$, this additional factor $\exp\{(\zeta \hat{b}^\dagger - \text{H.c.})t\}$ just generates a coherent state $|\alpha(t)\rangle$ of the photon field, whose amplitude $\alpha(t) = \zeta t$ grows linearly with time t .

The overlap of these coherent states at different times $\langle \alpha(t_1) | \alpha(t_2) \rangle = e^{-\zeta^2(t_1 - t_2)^2/2}$ modifies Eq. (4) via

$$P(t) = \int_0^t dt_1 \int_0^{t_1} dt_2 \int_F d^2k |\gamma_{\mathbf{k}}|^2 \exp\left\{-\frac{\zeta^2}{2}(t_1 - t_2)^2\right\} \times \exp\{-i(\epsilon_d - \epsilon_{\mathbf{k}})(t_1 - t_2)\}. \quad (14)$$

For very short times $t \ll T_*$ and $t \ll 1/\zeta$, we recover the initial quadratic growth in Eq. (5). What happens after that initial period depends on the quantity ζT_* . For small $\zeta T_* \ll 1$, we recover Eq. (7). For large $\zeta T_* \gg 1$, on the other hand, the probability is strongly suppressed,

$$P(t) \sim t \frac{\sqrt{2}}{\zeta} \int_F d^2k |\gamma_{\mathbf{k}}|^2, \quad (15)$$

which is a manifestation of the quantum Zeno effect by frequent measurements with the effective rate ζ .

The detector signal can be very explicitly evaluated with methods of full counting statistics or quantum polyspectra [24,44]. However, already the analysis of average values reveals (see Supplemental Material [37]) that, although delay effects occur, a transition between the timescales can be directly resolved.

Conclusions. For the example of a quantum dot tunnel coupled to an effectively two-dimensional electron reservoir, we study whether and how the quantum Zeno effect can be employed to suppress tunneling between a discrete level and a continuum. In contrast to tunneling between two discrete levels, we find that the required measurement repetition rate is set by the time T_* it takes the wave packet in the reservoir to

move away from the vicinity of the quantum dot. Hence this timescale can be increased (and thus the required repetition rate decreased) by lowering the Fermi energy or having a flat band (thus reducing the Fermi velocity) or by applying a strong perpendicular magnetic field, which effectively localizes the reservoir modes.

In a bigger picture, suppressing tunneling via the quantum Zeno effect and thereby effectively isolating the quantum dot from its environment is quite analogous to passive quantum-error-correcting schemes, such as the spin-echo method. In contrast to active quantum-error-correcting schemes (typically involving redundancies), such passive schemes are based on interrupting the coherence between the quantum dot or qubit and its environment such that the constructive interference of the error amplitudes is turned into a (at least partially) destructive interference. As an intuitive picture, these methods work well as long as the wave packet associated with the quantum error is still “lurking” in the vicinity of the quantum dot or qubit. Once they move too far away, the impact of measurements or echo sequences is strongly reduced.

As an outlook, frequent measurements can also enable or accelerate quantum evolution, which is usually referred to as the anti-Zeno effect [43]. As shown in the Supplemental Material [37], this effect can in principle also be realized in quantum dots, opening further windows for manipulation.

Experimental scenarios. In order to discuss the experimental relevance of our findings, let us insert typical experimental parameters. For an effective mass of around 7% of the electron mass [45] and a 2D electron density between 3 and $6 \times 10^{11} \text{ cm}^{-2}$, we get Fermi energies between 10 and 20 meV and Fermi velocities between 2 and $4 \times 10^5 \text{ m/s}$. Assuming a typical level spacing in the quantum dot of around 50 meV [34,45], the characteristic length scale of the ground-state wave function is $\ell \approx 5 \text{ nm}$. With a Fermi momentum of order 10^8 m^{-1} , we have $k_F \ell$ of order unity. Thus we may estimate the crossover time T_* by comparing the Fermi velocity with the length scale $\ell \approx 5 \text{ nm}$, which yields rather short times of order $T_* = \mathcal{O}(10 \text{ fs})$. Unfortunately, although measurements can be performed quite fast (on the nanosecond scale [20]), this $T_* = \mathcal{O}(10 \text{ fs})$ is probably too short to observe the quantum Zeno effect in this setup. Increasing this timescale T_* by decreasing the Fermi energy (i.e., reducing the electron density in the reservoir) or by using materials with a flat band is possible in principle but experimentally quite challenging.

Thus, probably the most viable option is to apply a strong perpendicular magnetic field B , say, of around 10 T, such that the 2DEG is in the quantum Hall regime [46]. In the quantum Hall regime, small residual electric fields within the 2DEG that originates, e.g., from interface roughness or electrostatic potential fluctuations introduced by the quantum dots will result in a drift of the wave packet in crossed E and B fields. The drift velocity $v_{\text{drift}} = c(\mathbf{E} \times \mathbf{B})$ is, however, much lower than the Fermi velocity in the original, field-free 2DEG. Thus the problem of a temporally decreasing overlap is diminished. The resulting magnetic length of $\ell_B \approx 8 \text{ nm}$ is roughly of the same order as the length scale $\ell \approx 5 \text{ nm}$ associated with the quantum dot, and similarly, the Landau-level spacing of about 15 meV is not too far away from the other energy scales. With aligning the energy levels accordingly, one can

arrange resonant tunnel transitions between the discrete level of the quantum dot and one of the discrete Landau levels in the reservoir. In this case, the line of arguments sketched in the Introduction can be applied, and thus the measurement repetition rate is set by the tunneling rate γ between these two levels. Since the time-associated scale $1/\gamma$ can be quite long (in the micro- to millisecond regime or even longer, which would also enable an electric readout [17,18]), a measurement time in the nanosecond regime should be sufficient to observe the quantum Zeno effect.

In order to enable such an observation, one has to make sure that the environmental decoherence (which can have basically the same effect as a measurement; for a review of tunneling in a dissipative environment see, e.g., [47]) is weak enough, i.e., the associated coherence time is longer than the time between measurements. A frequently discussed decoherence mechanism is the scattering of the electrons or holes in the reservoir at local impurities. As long as these impurities (which can be characterized experimentally [48]) are not too dense and thus far away from the dot, this mechanism is not relevant here because, as explained above, if the reservoir wave packet moved away from the dot far enough to see the impurity, it is already outside the region of applicability

of the quantum Zeno effect. Another potentially important mechanism stems from the Coulomb interaction between the electrons or holes or their interaction with phonons. In order to suppress this decoherence mechanism, the temperature should be low enough such that the available phase space and number of excitations is reduced.

Also in this respect, working in a strong magnetic field can be helpful: While electron-phonon scattering in a field-free 2DEG happens in two-dimensional k space, in the quantum Hall regime electron-phonon scattering is limited to the one-dimensional (both in real space and k space) lines along which the electrons drifts. This reduced dimensionality strongly suppresses electron-phonon scattering and renders it negligible at milli-Kelvin temperatures. At these temperatures T , electron-electron scattering is the only relevant mechanism and follows a T^2 law [49] in a 2DEG in a strong magnetic field. Experimental studies of the universality in the quantum Hall regime [50] allow one to estimate the associated timescale.

Acknowledgments. R.S. acknowledges valuable discussions with S. Popescu and W. G. Unruh. Funded by the Deutsche Forschungsgemeinschaft (DFG, German Research Foundation), Project ID No. 278162697-SFB 1242.

-
- [1] B. Misra and E. C. G. Sudarshan, The Zeno's paradox in quantum theory, *J. Math. Phys.* **18**, 756 (1977).
 - [2] W. M. Itano, D. J. Heinzen, J. J. Bollinger, and D. J. Wineland, Quantum Zeno effect, *Phys. Rev. A* **41**, 2295 (1990).
 - [3] G. Hackenbroich, B. Rosenow, and H. A. Weidenmüller, Quantum Zeno Effect and Parametric Resonance in Mesoscopic Physics, *Phys. Rev. Lett.* **81**, 5896 (1998).
 - [4] M. C. Fischer, B. Gutiérrez-Medina, and M. G. Raizen, Observation of the Quantum Zeno and Anti-Zeno Effects in an Unstable System, *Phys. Rev. Lett.* **87**, 040402 (2001).
 - [5] E. W. Streed, J. Mun, M. Boyd, G. K. Campbell, P. Medley, W. Ketterle, and D. E. Pritchard, Continuous and Pulsed Quantum Zeno Effect, *Phys. Rev. Lett.* **97**, 260402 (2006).
 - [6] J. Bernu, S. Deléglise, C. Sayrin, S. Kuhr, I. Dotsenko, M. Brune, J. M. Raimond, and S. Haroche, Freezing Coherent Field Growth in a Cavity by the Quantum Zeno Effect, *Phys. Rev. Lett.* **101**, 180402 (2008).
 - [7] D. H. Slichter, C. Müller, R. Vijay, S. J. Weber, A. Blais, and I. Siddiqi, Quantum Zeno effect in the strong measurement regime of circuit quantum electrodynamics, *New J. Phys.* **18**, 053031 (2016).
 - [8] P. Facchi, H. Nakazato, and S. Pascazio, From the Quantum Zeno to the Inverse Quantum Zeno Effect, *Phys. Rev. Lett.* **86**, 2699 (2001).
 - [9] P. Facchi and S. Pascazio, Quantum Zeno Subspaces, *Phys. Rev. Lett.* **89**, 080401 (2002).
 - [10] P. Facchi, D. A. Lidar, and S. Pascazio, Unification of dynamical decoupling and the quantum Zeno effect, *Phys. Rev. A* **69**, 032314 (2004).
 - [11] H. M. Wiseman and G. J. Milburn, *Quantum Measurement and Control* (Cambridge University Press, Cambridge, England, 2010).
 - [12] G. A. Álvarez, D. D. B. Rao, L. Frydman, and G. Kurizki, Zeno and Anti-Zeno Polarization Control of Spin Ensembles by Induced Dephasing, *Phys. Rev. Lett.* **105**, 160401 (2010).
 - [13] G. A. Paz-Silva, A. T. Rezakhani, J. M. Dominy, and D. A. Lidar, Zeno Effect for Quantum Computation and Control, *Phys. Rev. Lett.* **108**, 080501 (2012).
 - [14] F. Schäfer, I. Herrera, S. Cherukattil, C. Lovecchio, F. Cataliotti, F. Caruso, and A. Smerzi, Experimental realization of quantum Zeno dynamics, *Nat. Commun.* **5**, 3194 (2014).
 - [15] G. Barontini, L. Hohmann, F. Haas, J. Estève, and J. Reichel, Deterministic generation of multiparticle entanglement by quantum Zeno dynamics, *Science* **349**, 1317 (2015).
 - [16] B. Zhu, B. Gadway, M. Foss-Feig, J. Schachenmayer, M. L. Wall, K. R. A. Hazzard, B. Yan, S. A. Moses, J. P. Covey, D. S. Jin, J. Ye, M. Holland, and A. M. Rey, Suppressing the Loss of Ultracold Molecules Via the Continuous Quantum Zeno Effect, *Phys. Rev. Lett.* **112**, 070404 (2014).
 - [17] T. Fujisawa, T. Hayashi, R. Tomita, and Y. Hirayama, Bidirectional counting of single electrons, *Science* **312**, 1634 (2006).
 - [18] C. Flindt, C. Fricke, F. Hohls, T. Novotny, K. Netocny, T. Brandes, and R. J. Haug, Universal oscillations in counting statistics, *Proc. Natl. Acad. Sci. USA* **106**, 10116 (2009).
 - [19] A. Kurzman, B. Merkel, P. A. Labud, A. Ludwig, A. D. Wieck, A. Lorke, and M. Geller, Optical Blocking of Electron Tunneling into a Single Self-Assembled Quantum Dot, *Phys. Rev. Lett.* **117**, 017401 (2016).
 - [20] A. Kurzman, P. Stegmann, J. Kerski, R. Schott, A. Ludwig, A. D. Wieck, J. König, A. Lorke, and M. Geller, Optical Detection of Single-Electron Tunneling into a Semiconductor Quantum Dot, *Phys. Rev. Lett.* **122**, 247403 (2019).
 - [21] S. A. Gurvitz, L. Fedichkin, D. Mozyrsky, and G. P. Berman, Relaxation and the Zeno Effect in Qubit Measurements, *Phys. Rev. Lett.* **91**, 066801 (2003).

- [22] S. A. Gurvitz, Quantum limit of measurement and the projection postulate, *Int. J. Mod. Phys. B* **20**, 1363 (2006).
- [23] D. Segal and D. R. Reichman, Zeno and anti-Zeno effects in spin-bath models, *Phys. Rev. A* **76**, 012109 (2007).
- [24] G. Schaller, J. Cerrillo, G. Engelhardt, and P. Strasberg, Electronic Maxwell demon in the coherent strong-coupling regime, *Phys. Rev. B* **97**, 195104 (2018).
- [25] N. V. Leppen and D. S. Smirnov, Optical measurement of electron spins in quantum dots: Quantum Zeno effects, [arXiv:2202.13994](https://arxiv.org/abs/2202.13994).
- [26] S. A. Gurvitz, Measurements with a noninvasive detector and dephasing mechanism, *Phys. Rev. B* **56**, 15215 (1997).
- [27] G. Engelhardt and G. Schaller, Maxwell's demon in the quantum-Zeno regime and beyond, *New J. Phys.* **20**, 023011 (2018).
- [28] T. Ando, A. B. Fowler, and F. Stern, Electronic properties of two-dimensional systems, *Rev. Mod. Phys.* **54**, 437 (1982).
- [29] S. M. Reimann and M. Manninen, Electronic structure of quantum dots, *Rev. Mod. Phys.* **74**, 1283 (2002).
- [30] M. Russ, A. Lorke, D. Reuter, and P. Schafmeister, Self-assembled quantum dots as probes for Landau-level spectroscopy, *Physica E* **22**, 506 (2004).
- [31] M. Ruß, C. Meier, A. Lorke, D. Reuter, and A. D. Wieck, Role of quantum capacitance in coupled low-dimensional electron systems, *Phys. Rev. B* **73**, 115334 (2006).
- [32] M. Geller, Nonequilibrium carrier dynamics in self-assembled quantum dots, *Appl. Phys. Rev.* **6**, 031306 (2019).
- [33] E. E. Vdovin, A. Levin, A. Patanè, L. Eaves, P. C. Main, Y. N. Khanin, Y. V. Dubrovskii, M. Henini, and G. Hill, Imaging the electron wave function in self-assembled quantum dots, *Science* **290**, 122 (2000).
- [34] R. J. Warburton, B. T. Miller, C. S. Dürr, C. Bödefeld, K. Karrai, J. P. Kotthaus, G. Medeiros-Ribeiro, P. M. Petroff, and S. Huant, Coulomb interactions in small charge-tunable quantum dots: A simple model, *Phys. Rev. B* **58**, 16221 (1998).
- [35] O. S. Wibbelhoff, A. Lorke, D. Reuter, and A. D. Wieck, Magnetocapacitance probing of the many-particle states in InAs dots, *Appl. Phys. Lett.* **86**, 092104 (2005).
- [36] H. Haug and A.-P. Jauho, *Quantum Kinetics in Transport and Optics of Semiconductors* (Springer, Berlin, 2008).
- [37] See Supplemental Material at <http://link.aps.org/supplemental/10.1103/PhysRevResearch.4.L032045> for details on the dynamics of detectors sensitive to filled or empty dots, Zeno dynamics for reservoirs with a structured spectral function, and details on the inverse Zeno effect for off-resonant reservoirs [8,43,51–53].
- [38] R. Schützhold and G. Gnanapragasam, Quantum Zeno suppression of three-body losses in Bose-Einstein condensates, *Phys. Rev. A* **82**, 022120 (2010).
- [39] S. A. Gurvitz, Josephson-type effect in resonant-tunneling heterostructures, *Phys. Rev. B* **44**, 11924 (1991).
- [40] D. Zhou, A. Beckel, A. Ludwig, A. D. Wieck, M. Geller, and A. Lorke, Tuning the tunneling probability between low-dimensional electron systems by momentum matching, *Appl. Phys. Lett.* **106**, 243105 (2015).
- [41] O. Ciftja, Detailed solution of the problem of Landau states in a symmetric gauge, *Eur. J. Phys.* **41**, 035404 (2020).
- [42] W. Lei, C. Notthoff, J. Peng, D. Reuter, A. Wieck, G. Bester, and A. Lorke, “Artificial Atoms” in Magnetic Fields: Wave-Function Shaping and Phase-Sensitive Tunneling, *Phys. Rev. Lett.* **105**, 176804 (2010).
- [43] A. G. Kofman and G. Kurizki, Acceleration of quantum decay processes by frequent observations, *Nature (London)* **405**, 546 (2000).
- [44] M. Siffit, A. Kurzmann, J. Kerski, R. Schott, A. Ludwig, A. D. Wieck, A. Lorke, M. Geller, and D. Hägele, Quantum polyspectra for modeling and evaluating quantum transport measurements: A unifying approach to the strong- and weak-measurement regime, *Phys. Rev. Res.* **3**, 033123 (2021).
- [45] M. Fricke, A. Lorke, J. P. Kotthaus, G. Medeiros-Ribeiro, and P. M. Petroff, Shell structure and electron-electron interaction in self-assembled InAs quantum dots, *Europhys. Lett.* **36**, 197 (1996).
- [46] In the quantum Hall regime, small residual electric fields within the 2DEG that originate, e.g., from interface roughness or electrostatic potential fluctuations introduced by the quantum dots, will result in a drift of the wave packet in crossed \mathbf{E} and \mathbf{B} fields. The drift velocity $\mathbf{v}_{\text{drift}} = c(\mathbf{E} \times \mathbf{B})$ is, however, much lower than the Fermi velocity in the original, field-free 2DEG. Thus the problem of a temporally decreasing overlap is diminished.
- [47] A. Caldeira and A. Leggett, Quantum tunnelling in a dissipative system, *Ann. Phys.* **149**, 374 (1983).
- [48] J. Kerski, P. Lochner, A. Ludwig, A. Wieck, A. Kurzmann, A. Lorke, and M. Geller, Quantum Sensor for Nanoscale Defect Characterization, *Phys. Rev. Appl.* **15**, 024029 (2021).
- [49] B. L. Altshuler, A. B. Aronov, and D. E. Khmel'nitsky, Effects of electron-electron collisions with small energy transfers on quantum localisation, *J. Phys. C* **15**, 7367 (1982).
- [50] S. Koch, R. J. Haug, K. von Klitzing, and K. Ploog, Direct measurement of critical exponents in the quantum Hall regime, *Surf. Sci.* **263**, 108 (1992).
- [51] A. Nazir and G. Schaller, The reaction coordinate mapping in quantum thermodynamics, in *Thermodynamics in the Quantum Regime – Recent Progress and Outlook*, edited by F. Binder, L. A. Correa, C. Gogolin, J. Anders, and G. Adesso, *Fundamental Theories of Physics* (Springer, Cham, 2019), p. 551.
- [52] N. Martensen and G. Schaller, Transmission from reverse reaction coordinate mappings, *Eur. Phys. J. B* **92**, 30 (2019).
- [53] G. T. Landi, D. Poletti, and G. Schaller, Non-equilibrium boundary driven quantum systems: Models, methods and properties, *Rev. Mod. Phys.*, [arXiv:2104.14350](https://arxiv.org/abs/2104.14350).